 Bull. Chem. Soc. Jpn., **76**, 1329–1339 (2003)

Equation of State for Free Energy of Homogeneous Nucleation in Supersaturated Lennard-Jones Vapor Phase Derived by Monte Carlo Simulations

Yuri Yamada and Yosuke Kataoka*

Department of Materials Chemistry, College of Engineering, Hosei University,
3-7-2 Kajino-cho, Koganei, Tokyo 184-8584

(Received November 21, 2002)

We estimated the free energy of homogeneous nucleation in supersaturated Lennard-Jones vapor phase by using Monte Carlo simulations. The nucleation free energy of an N-particle cluster is obtained as the difference between the free energies of the cluster phase and the monomer phase in an N-particle system. In the previous papers, we estimated the Helmholtz free energy of the nucleation by MC calculations under a fixed volume per particle, $V/N = 43.2\ \sigma^3$, and the equation of state of the nucleation energy as a function of cluster size and temperature. In this study, we carried out some additional MC calculations under different volumes per particle and took into consideration the pressure to estimate the Gibbs free energy of the nucleation. Then we established the equations of state of the Helmholtz and Gibbs free energies of nucleation as a function of cluster size, temperature, and volume or pressure.

Homogeneous nucleation in supersaturated phase plays an important role as the starting point of phase transition. The critical nucleus, a diverging point for whether the generated cluster should grow or collapse, has been studied as to size and formation energy by various approaches.[1–7] In our previous papers,[8,9] we suggested a technique that estimates the Helmholtz free energy of homogeneous nucleation in supersaturated Lennard-Jones vapor phase by using Monte Carlo (MC) simulations under a fixed density, and we approximated the nucleation energy as an equation of state (EOS) that depends on the number of cluster particles and the temperature. In this study, we give the density dependence in the EOS with the results of new MC simulations for some additional volumes per particle. Moreover, we arrange the EOS to estimate the Gibbs free energy of the nucleation by taking into consideration the contribution of pressure.

Our model treats the N-particle nucleation as a phase transition between the cluster phase and the monomer phase in the N-particle system.[8,9] The former is a state in which all particles of the system construct a unified cluster, and the latter is a state in which all particles scatter as a supersaturated vapor. When the Helmholtz free energies of each phase for given numbers of particles N, volumes V, and temperatures T are obtained independently, the nucleation energy $\Delta A(N,T,V)$ can be estimated as:

$$\Delta A(N,T,V) = A^e_{\mathrm{c}}(N,T,V) - A^e_{\mathrm{m}}(N,T,V). \tag{1}$$

Here A^e_{c} and A^e_{m} are the interaction terms of the Helmholtz free energies of the cluster and monomer phases respectively. The interaction term of Helmholtz free energy $A^e(N,T,V)$ is estimated as:[10]

$$A^e(N,T,V) = U^e(N,T,V) - TS^e(N,T,V), \tag{2}$$

$$S^e(N,T,V) = \int_{T_0}^{T} \frac{(\partial U^e/\partial T)_{NV}}{T}\,\mathrm{d}T + S^e(N,T_0,V). \tag{3}$$

Here U^e is an averaged interaction energy of the system at each temperature. The interaction term of entropy S^e is estimated by the thermodynamic integration as the difference from the entropy at an origin temperature of T_0. Equations 1–3 treat only the interaction terms while neglecting the ideal gas terms. The ideal gas terms of the Helmholtz free energy on (N,T,V) domain are constant irrespective of the configuration of the system; therefore the ideal gas terms are canceled by the subtraction of Eq. 1.

On the other hand, the Gibbs free energy is sum of the Helmholtz free energy and the pressure term:

$$G = A + PV. \tag{4}$$

The Gibbs free energy of the nucleation should be obtained under constant pressure as

$$\begin{aligned}\Delta G(N,T,P) &= G_{\mathrm{c}}(N,T,P) - G_{\mathrm{m}}(N,T,P)\\ &= G_{\mathrm{c}}(N,T,V_{\mathrm{c}}) - G_{\mathrm{m}}(N,T,V_{\mathrm{m}}),\end{aligned} \tag{5}$$

where V_{c} and V_{m} are volumes of the cluster and monomer phases that present an identical pressure P. In this equation, the ideal gas terms of the each phase are not canceled because the ideal gas term of the Gibbs free energy depends on volume. Accordingly, to obtain the ΔG on (N,T,P) domain, the ideal gas terms G^{id}_{c} and G^{id}_{m} should be taken into account as

Published on the web July 15, 2003; DOI 10.1246/bcsj.76.1329

$$\Delta G(N,T,P) = \{G_c^{id}(N,T,V_c) + G_c^e(N,T,V_c)\} - \{G_m^{id}(N,T,V_m) + G_m^e(N,T,V_m)\}. \quad (6)$$

Monte Carlo Simulation

The simulation procedure is explained here. We applied Lennard-Jones (LJ) 12-6 type function for two-body interaction, and used the LJ parameters for reduced units of length σ, energy ε; temperature ε/k, with k being the Boltzmann constant; volume σ^3; pressure ε/σ^3. The first stage of the simulation is the cluster stabilization process. The distorted face-centered cubic lattice was prepared as an initial configuration.[8,9] Starting with the initial lattice, the system was cooled from 0.20 to 0.01 ε/k by 0.01 ε/k steps, where at least N million MC trial movements were performed for equilibration and statistics at each temperature. A stabilized cluster is obtained in this stage. Two ways of MC calculations were performed from the stabilized cluster: namely, phase transition calculation and cluster phase calculation. In the phase transition calculation, the system was heated from 0.01 to 1.00 ε/k. The cluster collapsed and evaporated to the monomer phase at a certain temperature that depends on the number of particles. The temperature interval was 0.01 ε/k, and we performed N million MC trials for equilibration and statistics at each temperature. On the other hand, in the cluster phase calculation, the cluster evaporation was prohibited even if the system was heated as in the phase transition calculation. After each MC movement, the new configuration is judged depending on whether all particles of the system belong to a cluster. The movement is canceled if the new configuration is not regarded as a cluster. We applied Stillinger's cluster criterion as the cluster decision: two particles are regarded to connect if their center-center distance is less than a threshold value, and the system configuration is regarded as the cluster phase if all the particles of the system are mutually connected.[11] We decided the threshold distance as 1.5 σ, that corresponds to the first minimum of the pair correlation function of the stabilized cluster. The superheated cluster is observed above the evaporation temperature.[8,9] In this manner, we performed the simulations for 128 states: $V/N = 30$, 43.2, 90, 240, and 1000 σ^3, and $N = 2$–80. Figure 1 shows the simulated states concretely.

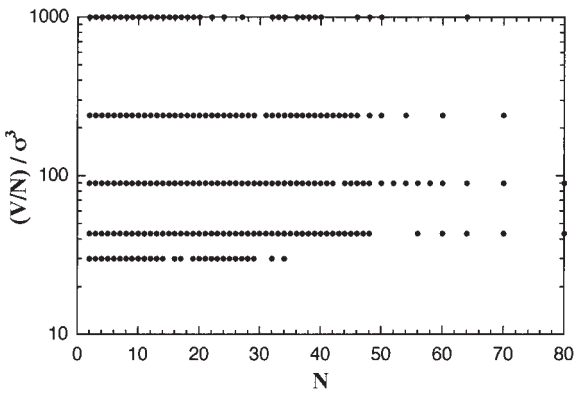

Fig. 1. Map of the simulated states in $(N, V/N)$ plane.

Equation of State

Monomer Phase. In the previous study, we confirmed that the interaction energy and the interaction entropy of the monomer phase do not depend on temperature. Thus these values can be assumed as the equilibrated values of the evaporated monomer phase in the phase transition calculation. A similar assumption can be adopted for pressure. Figure 2 shows the temperature dependence of an interaction term of pressure, $P^e = P - NkT/V$, in the phase transition calculation. Since the P^e levels off against temperature after the evaporation, we assume the equilibrated value into the P^e of the monomer phase.

On the assumption of the uniform distribution of particles in the monomer phase, the interaction energy per particle can be explained as

$$\frac{U_m^e}{N} = 4\pi\rho \int \phi(r) r^2 \mathrm{d}r, \quad (7)$$

where $\rho = N/V$ is the number density of the system. Accordingly, the interaction energy is predicted to be in proportion to

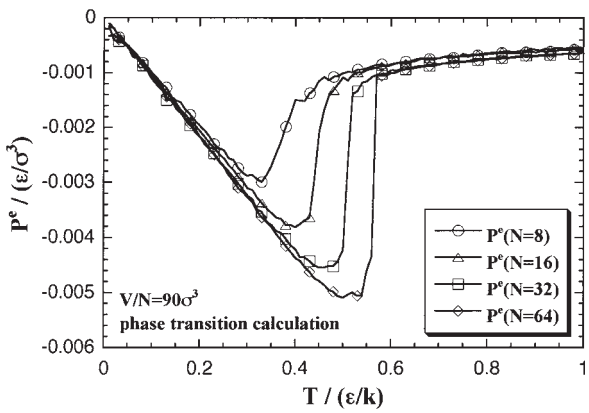

Fig. 2. Temperature dependence of the interaction term of pressure of the phase transition calculation at $V/N = 90$ σ^3. The curves leveled off after decomposition of the cluster.

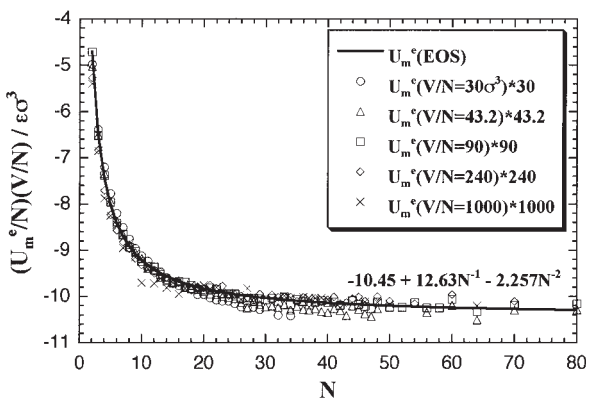

Fig. 3. The product of the interaction energy per particle of the monomer phase and the volume per particle. The circles, triangles, squares, diamonds and crosses show the MC result. The solid curve shows the result of the least-squares fitting by Eq. 12.

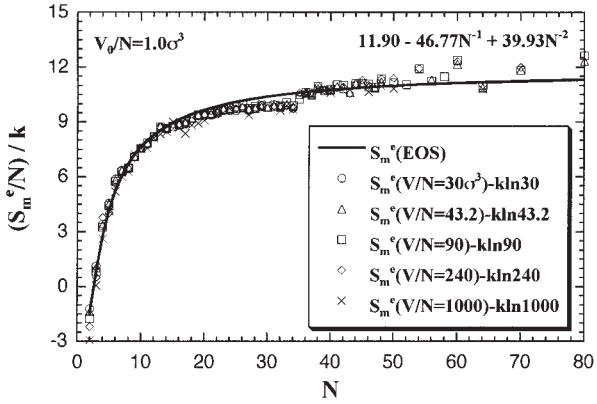

Fig. 4. The interaction term of entropy of the monomer phase is converted into the standard value of $V_0/N = 1.0\ \sigma^3$. The solid curve shows the result of the least-squares fitting by Eq. 13.

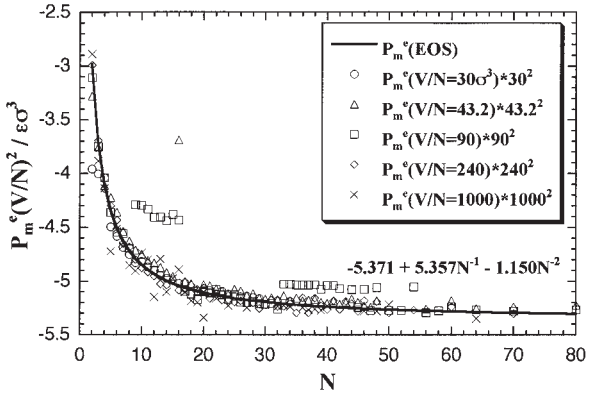

Fig. 5. The product of P_m^e and $(V/N)^2$ vs N plots. The solid curve shows the result of the least-squares fitting by Eq. 14.

the density. The product of the interaction energy per particle of the monomer phase and V/N on each density is plotted in Fig. 3. Secondly, the ideal gas equation of state obtains the entropy change of isothermal expansion ΔS_{exp} from volume V_0 to V as

$$\Delta S_{exp} = Nk \ln(V/V_0). \tag{8}$$

Here, when we set a standard value as $V_0/N = 1.0\ \sigma^3$, the expansion entropy is explained as

$$\Delta S_{exp} = Nk \ln(V/N\sigma^3); \tag{9}$$

then the interaction entropy of the monomer phase at V/N is predicted as a function of N and V/N,

$$S_m^e(N, V/N) = S_m^e(N, V_0/N) + Nk \ln(V/N\sigma^3). \tag{10}$$

Figure 4 shows the values that result when $k \ln(V/N\sigma^3)$ is subtracted from the interaction entropy per particle of the monomer phase for each density. Lastly, we consider the van der Waals equation to predict the V/N dependence of pressure of the monomer phase. That is,

$$P = \frac{NkT}{V - Nb} - a\rho^2, \tag{11}$$

where a and b are the van der Waals coefficients. The first term indicates the ideal gas term and a repulsive part of the interaction term, and the second term is an attractive part. In the monomer phase, the interaction is almost occupied by the attractive part because the particles are scattered in the system. That is to say, the interaction term of pressure is predicted to be in proportion to the square of ρ. The product of the interaction term of the pressure of the monomer phase and the square of the volume per particle is plotted in Fig. 5.

On the basis of the above considerations, we defined approximated functions for the interaction energy, the interaction terms of entropy, and pressure of the monomer phase. The functions were designed as the power series:[12,13]

Table 1. Results of Least-squares Fittings for the Monomer Phase, a_i, b_i, and c_i

i	a_i	b_i	c_i
0	−1.045E+01	1.190E+01	−5.371E+00
1	1.263E+01	−4.677E+01	5.357E+00
2	−2.257E+00	3.993E+01	−1.150E+00

E+01 means 10^1.

$$\frac{U_m^e}{N} = \left\{\sum_{i=0}^{2} a_i N^{-i}\right\} \Big/ (V/N), \tag{12}$$

$$\frac{S_m^e}{N} = \left\{\sum_{i=0}^{2} b_i N^{-i}\right\} + k \ln(V/N), \tag{13}$$

$$\frac{P_m^e V}{N} = \left\{\sum_{i=0}^{2} c_i N^{-i}\right\} \Big/ (V/N). \tag{14}$$

The pressure term was treated as $P_m^e V$ per particle to coordinate with U_m^e and S_m^e. The coefficients a_i, b_i, and c_i were obtained respectively by least-squares fittings. Table 1 and Figs. 3–5 show the fitting results, the coefficients and the fitted curves. When we decide the relative deviation of the thermodynamic property X to be

$$\delta' X = \frac{\langle [\delta X]^2 \rangle^{1/2}}{\langle X^2 \rangle^{1/2}}, \tag{15}$$

then $\delta'(U_m^e/N) = 0.0169$, $\delta'(S_m^e/N) = 0.0304$, $\delta'(P_m^e V/N) = 0.00822$.

Cluster Phase. The density dependence of U_c^e, S_c^e, and $P_c^e V$ of the cluster phase is mentioned below. In the cluster phase calculation, all particles of the system were restricted through high temperature to keep a unity cluster by Stillinger's cluster criterion. Now, the criterion focuses only on the interparticle distance, so the shape of the cluster is not considered.[5,14] Therefore, if the configuration satisfies only the criterion of the interparticle distance, the configuration is permitted as a cluster even though the configuration is collapsed and stretched by heating, like Fig. 6. The stretched clusters appear frequently when the number of particle becomes larger or the density smaller. On the contrary, we found in our simula-

Fig. 6. An example snapshot of the stretched cluster on the cluster phase calculation: $N = 50$, $V/N = 1000\ \sigma^3$, and $T = 1.00\ \varepsilon/k$. This configuration satisfies the Stillinger's cluster criterion.

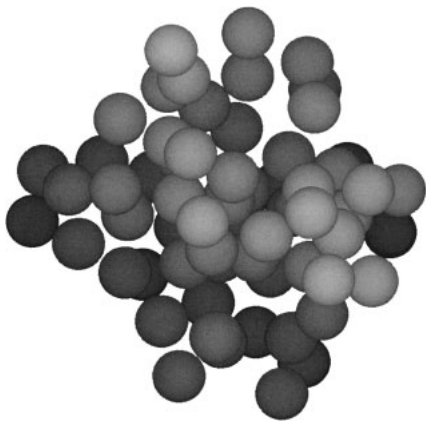

Fig. 7. An example snapshot of the stable spherical cluster on the cluster phase calculation: $N = 64$, $V/N = 90\ \sigma^3$, and $T = 1.00\ \varepsilon/k$.

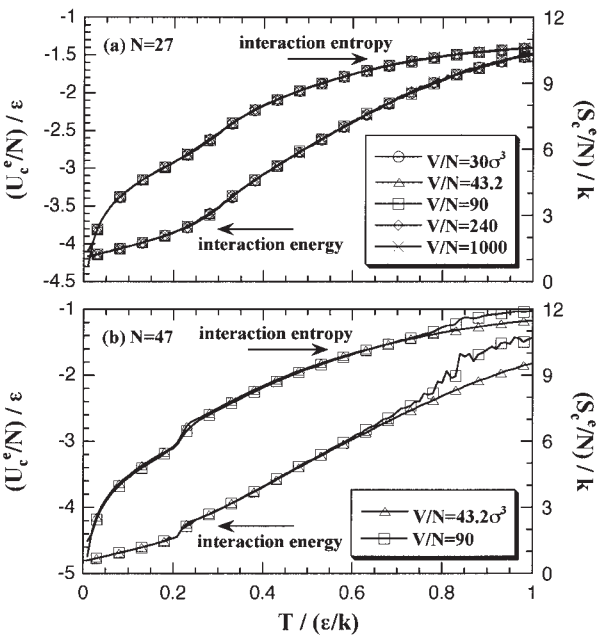

Fig. 8. Density dependence of the interaction energy and the interaction entropy of the cluster phase. The 27-particle systems (a) obtain spherical cluster phases on each volume per particle, so there is no dependence on the density. However, in the 47-particle systems (b), the U_c^e and S_c^e have disagreement at high temperature because the stretched cluster is obtained in $V/N = 90\ \sigma^3$.

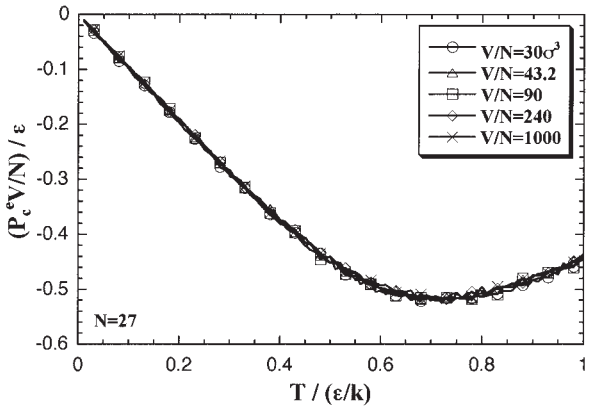

Fig. 9. Density dependence of the P_c^eV term of 27-particle system of the cluster phase. Similar to Fig. 8(a), there is no dependence on the density.

tions a tendency that the cluster keeps the spherical shape through the high-temperature under the specific numbers of particles; $N = 27$, 32, 34, and 64. We surmise that it is similar to a Magic Number for clusters: i.e., the specific number of particles that can form a rather stable cluster.[15] An example of the stable configuration of 64-particle cluster at $1.00\ \varepsilon/k$ is shown in Fig. 7.

In our model, the cluster phase contains an N-particle cluster and no vapor phase particles in the surroundings of the cluster. Since the system has no interaction between cluster-vapor or cluster-cluster, if the shape of cluster was similarly spherical, there would be no dependence on the system density in U_c^e, S_c^e, and P_c^eV; such examples of the 27-particle system are shown in Figs. 8a and 9. However, the stretched cluster has disagreements in U_c^e, S_c^e, and P_c^eV with the spherical cluster; an example of the 47-particle system is shown in Fig. 8b.

The interaction entropy of the cluster phase is obtained by the thermodynamic integration of the interaction energy as Eq. 3. Therefore, the interaction energy and the interaction entropy should be approximated essentially by one function for the interaction energy. However, in the previous study, we were obliged to approximate the interaction energy and the interaction entropy separately. The dispersion of the interaction energy that was due to the appearance of the stretched cluster caused the approximation by one function to be unsuccessful. Accordingly, in this study, we remove the stretched clusters from the subjects of the approximation and attempt to approximate the U_c^e and S_c^e as one function. The approximated functions for the U_c^e and the P_c^eV term of the cluster phase are power series of temperature and number of particles:[12,13]

$$\frac{U_c^e}{NT} = \sum_m \sum_n \{a_{mn} N^m T^n\}, \quad (m = -3, -2, -1, 0, 1, 2; n = -1, 0, 1, 2, 3, 4) \tag{16}$$

$$\frac{P_c^e V}{N} = \sum_p \sum_q \{b_{pq} N^p T^q\}. \quad (p = -3, -2, -1, 0; q = 0, 1, 2, 3, 4) \tag{17}$$

The approximation of Eq. 16 is performed as (U_c^e/NT) for the

Table 2. Results of Least-squares Fittings for the Cluster Phase, a_{mn} and b_{pq}

a_{mn}	m: 2	1	0	−1	−2	−3	b_{pq}	p: 0	−1	−2	−3
4	3.125E−02	−3.424E+00	1.222E+02	−1.027E+03	2.937E+03	−2.713E+03	5	−5.208E+00	1.023E+02	−3.426E+02	3.161E+02
3	−6.758E−02	7.527E+00	−2.735E+02	2.417E+03	−7.041E+03	6.540E+03	4	1.332E+01	−3.012E+02	1.106E+03	−1.106E+03
2	4.536E−02	−5.156E+00	1.899E+02	−1.831E+03	5.491E+03	−5.142E+03	3	−1.080E+01	2.958E+02	−1.191E+03	1.269E+03
1	−9.449E−03	1.100E+00	−3.813E+01	4.436E+02	−1.400E+03	1.325E+03	2	3.496E+00	−1.059E+02	4.739E+02	−5.364E+02
0	4.015E−04	−4.656E−02	3.000E+00	−2.137E+01	5.442E+01	−4.490E+01	1	−1.425E+00	1.421E+01	−6.355E+01	7.562E+01
−1	8.790E−05	−2.183E−02	−4.362E+00	2.075E+01	−4.375E+01	3.581E+01	0	9.166E−03	−3.736E−01	1.869E+00	−2.337E+00

n

q

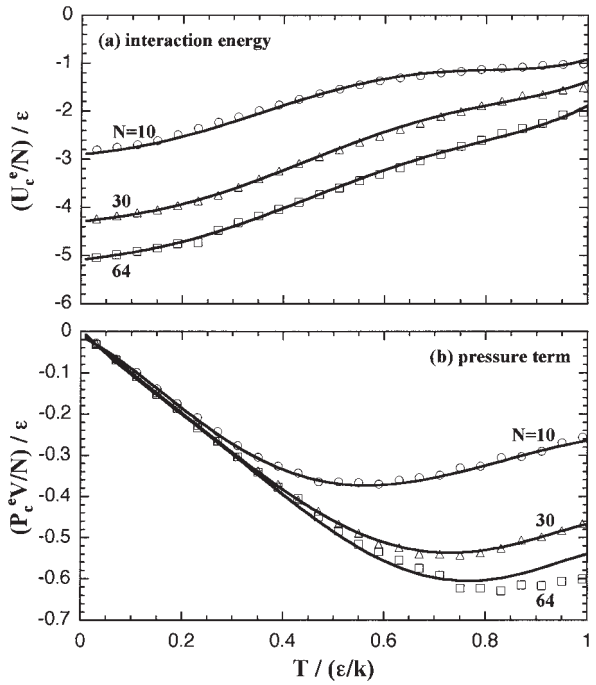

Fig. 10. Fitting results of the cluster phase; (a) the interaction energy, and (b) the product of the interaction term of pressure and volume. Circles, triangles, and squares are the MC results while the curves are the EOS. Care should be taken that the approximated functions for the cluster phase, Eqs. 16 and 17, have no dependence on the volume per particle.

purpose of fitting accuracy. After the least squares fittings, we obtained the coefficients a_{mn} and b_{pq} as shown in Table 2 and the curves as shown in Figs. 10 and 11. The relative deviations are $\delta'(U_c^e/NT) = 0.0190$ and $\delta'(P_c^eV/N) = 0.0327$. Incidentally, the relative deviations of the interaction entropy, and of the interaction terms of Helmholtz and Gibbs free energy of the cluster phase are $\delta'(S_c^e/T) = 0.0547$, $\delta'(A_c^e/T) = 0.0357$, and $\delta'(G_c^e/N) = 0.0343$.

Nucleation Energy. Helmholtz free energy of nucleation ΔA on (N, T, V) domain is obtained by Eq. 1. In Fig. 12, we compare the ΔA obtained from the EOS and the results of MC simulations. Figure 13 shows the critical values, the size N_A^* and the nucleation energy ΔA^*, that are obtained from the maximum of a nucleation energy curve like Fig. 12. On the other hand, as we mentioned above, the Gibbs free energy of the nucleation should be obtained under constant pressure and the ideal gas term should be included in the process of obtaining ΔG, like Eq. 6. To make a relationship between the simulation results and the ideal gas, we assumed that the thermodynamic properties of the monomer phase resemble those of the ideal gas. We obtain the ΔG on (N, T, P) domain with the following procedure.

An interaction term of the Helmholtz free energy of the monomer phase can be obtained by the density integration of the compressibility factor at each number of particles as ${}_zA_m^e$:[13]

$$\frac{\beta {}_zA_m^e}{N} = \int_0^\rho \left(\frac{\beta P}{\rho} - 1\right)\frac{1}{\rho}\mathrm{d}\rho, \quad \beta = \frac{1}{kT}. \tag{18}$$

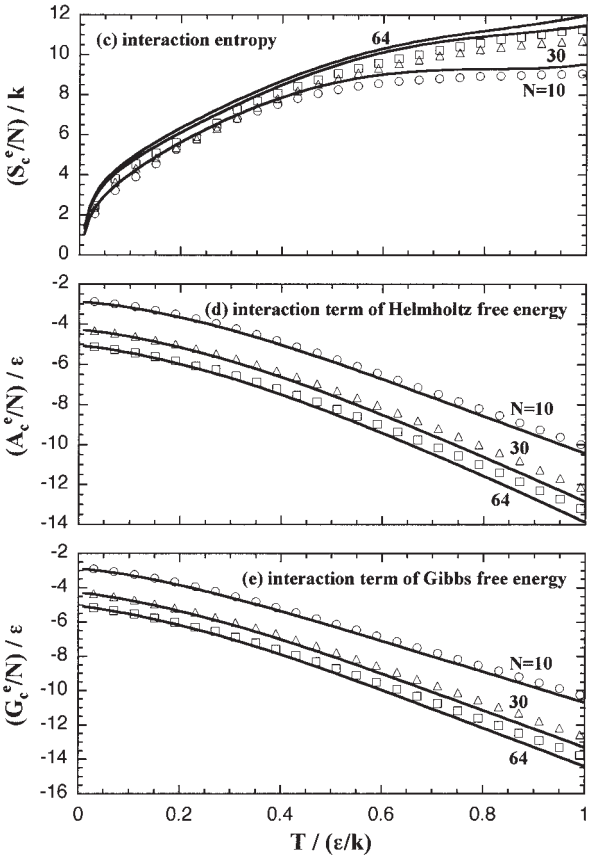

Fig. 11. Thermodynamic properties of the cluster phase that is derived from U_c^e and $P_c^e V$ with Eqs. 2–4; (c) the interaction entropy, (d) the interaction term of the Helmholtz free energy, and (e) one of the Gibbs free energy.

From the relation of $(\beta P/\rho - 1) = \beta P_m^e/\rho$ and the approximated function for the $P_m^e V$ of Eq. 14,

$$\frac{{}_Z A_m^e(N, V_m)}{N} = \left\{ \sum_{i=0}^{2} c_i N^{-i} \right\} \Big/ (V_m/N). \tag{19}$$

This re-estimates the interaction term of Gibbs free energy of the monomer phase $G_m^e(N, T, V_m)$. On the other hand, the interaction term of the Gibbs free energy of the cluster phase, $G_c^e(N, T, V_c)$, is obtained as

$$G_c^e(N, V_c, T) = U_c^e(N, T) - TS_c^e(N, V_c, T) + P_c^e V_c(N, T), \tag{20}$$

$$\begin{aligned} S_c^e(N, V_c, T) &= {}_Z S_m^e(N, V_c, T) + {}_{EOS}\Delta S^e(N, V_c, T) \\ &= \frac{{}_{EOS}U_m^e(N, V_c) - {}_Z A_m^e(N, V_c)}{T} \\ &\quad + \{{}_{EOS}S_c^e(N, T) - {}_{EOS}S_m^e(N, V_c)\}. \end{aligned} \tag{21}$$

Here, we obtain the interaction entropy of the cluster phase $S_c^e(N, T, V_c)$ as a sum of the interaction entropy of the monomer phase and the entropy change between the cluster and monomer phases: the former ${}_Z S_m^e$ is estimated from the compressibility factor in Eq. 19, and the latter ${}_{EOS}\Delta S^e$ is estimated from the approximated functions in Eqs. 13, 16, and 3. The ideal gas term of the Gibbs free energy G^{id} is defined by the statistical thermodynamics as:

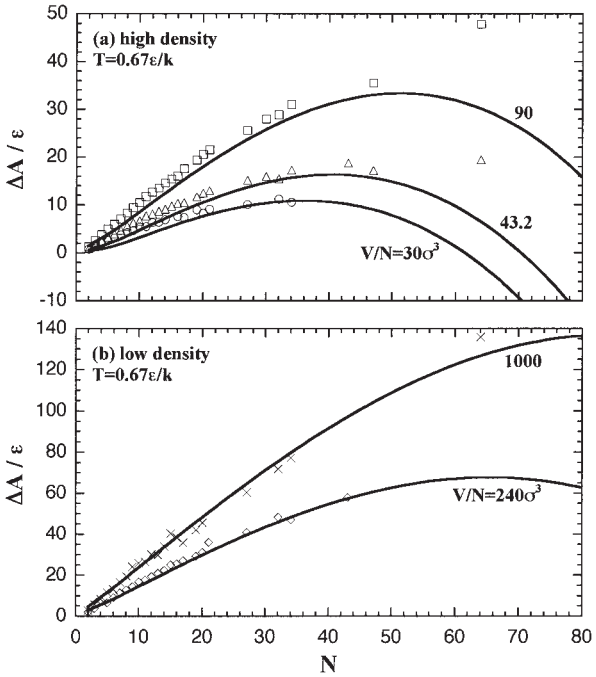

Fig. 12. Helmholtz free energy of the homogeneous nucleation on (N, T, V) domain at $T = 0.67\ \varepsilon/k$. The curves at high-density region, $V/N = 30$, 43.2, and 90 σ^3, are plotted in the upper figure (a), and low-density in the lower (b). Circles, triangles, squares, diamonds, and crosses are the MC results while the curves are the EOS.

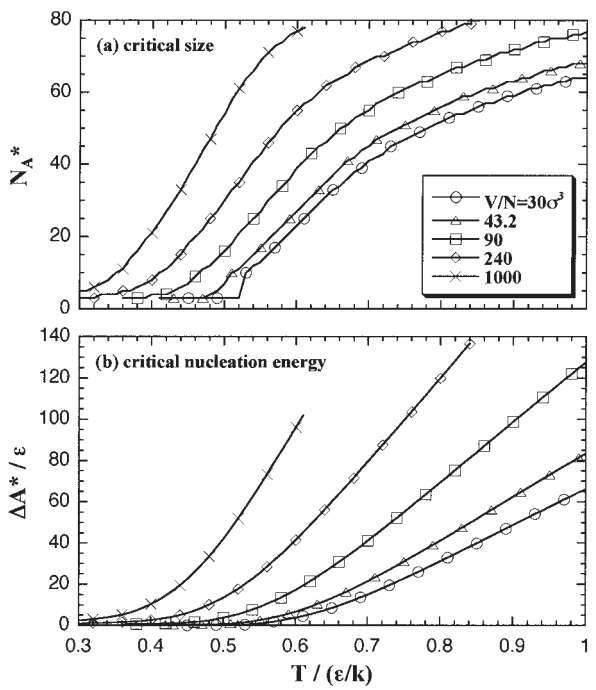

Fig. 13. The values of the critical nucleus in (N, T, V) domain: (a) the size N_A^* and (b) the Helmholtz free energy ΔA^*.

Table 3. Examples of the Concrete Values that Construct the Nucleation Energy at $T = 0.67\ \varepsilon/k$, $N = 32$, while $P = 0.0127$, 0.00679, and 0.00270 ε/σ^3

$P/(\varepsilon/\sigma^3)$		$(V/N)/\sigma^3$		U/ε	S/k	PV/ε	G/ε
1.27E−02	cluster	4.34E+01	ideal	4.12E+01	5.09E+02	2.75E+01	−2.73E+02
			interaction	−1.05E+02	−1.45E+02	−2.29E+01	−3.07E+01
	monomer	1.04E+01	ideal	4.12E+01	5.80E+02	2.75E+01	−3.20E+02
			interaction	−4.62E+00	−3.33E+00	−2.39E+00	−4.77E+00
	delta	3.29E+01	ideal	0.00E+00	−7.02E+01	0.00E+00	4.70E+01
			interaction	−1.00E+02	−1.41E+02	−2.06E+01	−2.60E+01
6.79E−03	cluster	9.01E+01	ideal	4.72E+01	5.80E+02	3.15E+01	−3.10E+02
			interaction	−1.27E+02	−1.70E+02	−2.68E+01	−4.03E+01
	monomer	1.95E+01	ideal	4.72E+01	6.65E+02	3.15E+01	−3.67E+02
			interaction	−5.32E+00	−3.84E+00	−2.75E+00	−5.49E+00
	delta	7.07E+01	ideal	0.00E+00	−8.50E+01	0.00E+00	5.69E+01
			interaction	−1.22E+02	−1.66E+02	−2.40E+01	−3.48E+01
2.70E−03	cluster	2.40E+02	ideal	3.22E+01	4.32E+02	2.14E+01	−2.36E+02
			interaction	−7.27E+01	−1.29E+02	−1.72E+01	−3.58E+00
	monomer	4.90E+01	ideal	3.22E+01	4.83E+02	2.14E+01	−2.70E+02
			interaction	−1.34E+00	−9.66E−01	−6.94E−01	−1.39E+00
	delta	1.91E+02	ideal	0.00E+00	−5.09E+01	0.00E+00	3.41E+01
			interaction	−7.14E+01	−1.28E+02	−1.65E+01	−2.19E+00

$$
\begin{aligned}
G^{id} &= U^{id} + P^{id}V - TS^{id},\\
U^{id} &= \frac{3}{2}NkT, \quad P^{id}V = NkT,\\
S^{id} &= \frac{U^{id}}{T} + Nk\ln q - k\ln N!,\\
q &= \frac{V}{\Lambda^3}, \quad \Lambda = \frac{h}{\sqrt{2\pi mkT}}.
\end{aligned}
\tag{22}
$$

Here the symbols q, Λ, h, and m indicate the molecular partition function, the thermal wavelength, Planck's constant, and the mass of the particle. We obtained the S^{id} with the LJ parameters and the mass of argon molecule, as $\varepsilon/k = 119.8$ K, $\sigma = 0.340$ nm, and $m = 6.634 \times 10^{-26}$ kg. Volumes of the cluster and the monomer phases, V_c and V_m, that present the identical pressure P, are obtained from Eqs. 14 and 17 as:

$$
\begin{aligned}
P &= \frac{f_m}{(V_m/N)^2} + \frac{kT}{(V_m/N)} = \frac{f_c + kT}{(V_c/N)},\\
f_m &= \sum_{i=0}^{2} c_i N^{-i}, \quad f_c = \sum_{p=-3}^{0}\sum_{q=0}^{4} b_{pq}N^p T^q.
\end{aligned}
\tag{23}
$$

The V_m/N and V_c/N at some pressures, 0.0127, 0.00679, and 0.00270 ε/σ^3, are plotted in Fig. 14. In the case of $P = 0.0679\ \varepsilon/\sigma^3$, the V_m/N is roughly constant at 90 σ^3, while the V_c/N changes from 90.6 σ^3 at $N = 2$ to 10.4 σ^3 at $N = 80$. However, at a low temperature, ca. $T < 0.4\ \varepsilon/k$ in the case of $P = 0.00680\ \varepsilon/\sigma^3$, the V_m/N values are not available: V_m/N is obtained from Eq. 23 by the quadratic formula, yet the square root term, $(kT)^2 + 4f_mP$, becomes negative at such low temperatures.

The above equations yield the Gibbs free energy of the nucleation on (N, T, P) domain with Eq. 6. Figure 15 shows the $\Delta G(N, T, P)$, and Table 3 shows the components of $\Delta G(N, T, P)$ concretely. In the high-density (high-pressure) region, Fig. 15(a), the ΔG curves are somewhat overestimated;

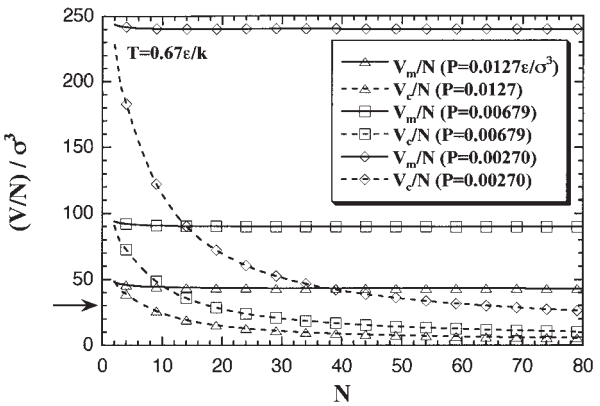

Fig. 14. Volumes per particle of the monomer and cluster phase at $T = 0.67\ \varepsilon/k$; that are obtained from Eq. 23. The pressure in LJ reduced units corresponds as $1\ \varepsilon/\sigma^3 = 41.9$ MPa in the case of argon. The arrow indicates a minimum of the simulated volume per particle as 30 σ^3; the volumes per particle of the cluster phase (dashed curves) are extrapolated at the figured pressures.

the value seems to have risen excessively at the large-N region. On the other hand, the curves of the low-density (low-pressure) region, Fig. 15(b), are lower than the curves of ΔA on corresponding volumes per particle. This can be explained as the following behavior of the components of ΔG and ΔA:

$$
\begin{aligned}
\Delta G(N,T,P) &= \Delta H_G(N,T,P) - T\Delta S_G(N,T,P)\\
&= \Delta U_G(N,T,P) + P\Delta V_G(N,T,P)\\
&\quad - T\Delta S_G(N,T,P),
\end{aligned}
\tag{24}
$$

$$
\Delta A(N,T,V) = \Delta U_A(N,T,V) - T\Delta S_A(N,T,V). \tag{25}
$$

First, we compare the internal energy term of the Gibbs free

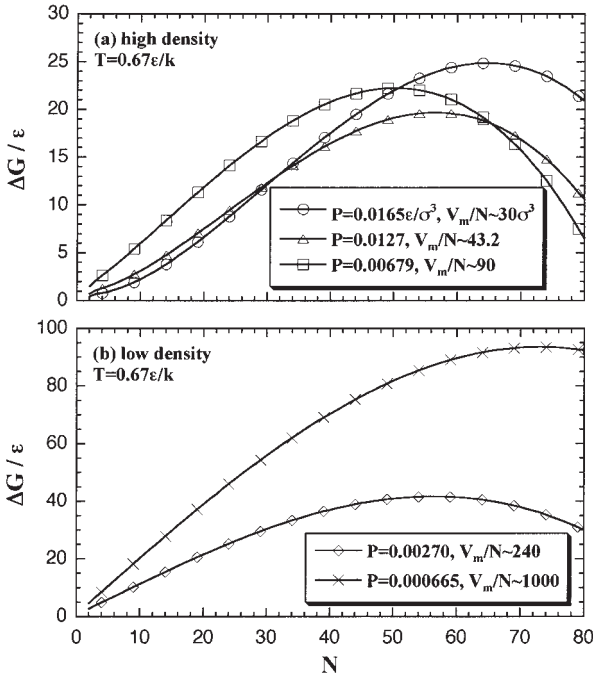

Fig. 15. Gibbs free energy of the homogeneous nucleation on (N, T, P) domain. The contribution of the ideal gas term is taken into consideration of the ΔG estimation. The volumes per particle of the monomer phase are mostly close to the figured values at the each maximum.

energy of the nucleation $\Delta U_G(N, T, P)$ and the one of the Helmholtz free energy $\Delta U_A(N, T, V_m)$ as:

$$\begin{aligned}\Delta U_G(N,T,P) &= \{U_c^e(N,T) - U_m^e(N,V_m)\} \\ &\quad + \{U_c^{id}(N,T) - U_m^{id}(N,T)\}, \\ \Delta U_A(N,T,V_m) &= U_c^e(N,T) - U_m^e(N,V_m),\end{aligned} \tag{26}$$

where the volume V_m gives the constant pressure P. The ideal gas term and the approximated function for the cluster phase have no dependence on volume per particle, as seen in Eqs. 22 and 16. Therefore, the internal energy terms of ΔU_G and ΔU_A are identical, irrespective of the volume per particle of the cluster phase. Secondly, the entropy terms, $\Delta S_G(N, T, P)$ and $\Delta S_A(N, T, V_m)$, are related in detail as:

$$\begin{aligned}\Delta S_G(N,T,P) &= \{S_c^e(N,T,V_c) - S_m^e(N,T,V_m)\} \\ &\quad + \{S_c^{id}(N,T,V_c) - S_m^{id}(N,T,V_m)\}, \\ S_c^e(N,T,V_c) &= \frac{{}_{EOS}U_m^e(N,V_c) - {}_{Z}A_m^e(N,V_c)}{T} \\ &\quad + \{{}_{EOS}S_c^e(N,T) - {}_{EOS}S_m^e(N,V_c)\}, \\ S_m^e(N,T,V_m) &= \frac{{}_{EOS}U_m^e(N,V_m) - {}_{Z}A_m^e(N,V_m)}{T}, \\ S_c^{id}(N,T,V_c) - S_m^{id}(N,T,V_m) &\\ = Nk\left\{\ln\frac{V_c}{\Lambda^3} - \ln\frac{V_m}{\Lambda^3}\right\} &= Nk\ln\frac{V_c}{V_m}, \quad \text{and} \\ \Delta S_A(N,T,V_m) &= {}_{EOS}S_c^e(N,T) - {}_{EOS}S_m^e(N,V_m).\end{aligned} \tag{27}$$

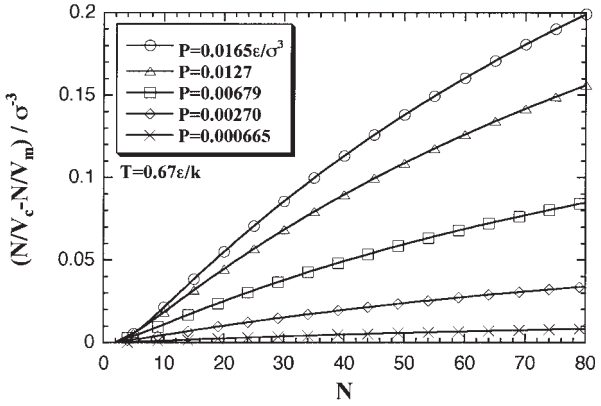

Fig. 16. Pressure dependence of the density term of the contribution of the entropy term toward the difference between $\Delta G(N, T, P)$ and $\Delta A(N, T, V_m)$. When the pressure becomes lower (V_m/N larger), the density term and Eq. 29 become smaller.

The expressions can be rearranged by Eqs. 12, 13, and 19,

$$\begin{aligned}&T\Delta S_G(N,T,P) \\ &= N\left\{\sum a_i N^{-i} - \sum c_i N^{-i}\right\}\{N/V_c - N/V_m\} \\ &\quad + T_{EOS}S_c^e(N,T) - NT\left\{\sum b_i N^{-i} + k\ln(V_c/N)\right\} \\ &\quad + NkT\ln(V_c/V_m), \quad \text{and} \\ &T\Delta S_A(N,T,V_m) \\ &= T_{EOS}S_c^e(N,T) - NT\left\{\sum b_i N^{-i} + k\ln(V_m/N)\right\}.\end{aligned} \tag{28}$$

Their difference is

$$\begin{aligned}&T\Delta S_G(N,T,P) - T\Delta S_A(N,T,V_m) \\ &= N\left\{\sum a_i N^{-i} - \sum c_i N^{-i}\right\}\{N/V_c - N/V_m\}.\end{aligned} \tag{29}$$

This explains the contribution of the entropy term toward the difference between $\Delta G(N, T, P)$ and $\Delta A(N, T, V_m)$. The density term of Eq. 29, $N/V_c - N/V_m$, is nearly in proportion to the pressure, i.e., becomes larger in the smaller V_m/N system as in Fig. 16. In the case of high-pressure and small-V_m/N system, the density of the cluster phase becomes somewhat higher: $V_c/N \sim 4.3\ \sigma^3$ at $P = 0.0165\ \varepsilon/\sigma^3$, $N = 80$, and $T = 0.67\ \varepsilon/k$. From the MC results of $V_c/N = 30$ up to $1000\ \sigma^3$, we assumed that the thermodynamic properties of the cluster phase, U_c^e, S_c^e, and $P_c^e V_c$, do not depend on the density such as Eqs. 16 and 17. However, it is not guaranteed that the thermodynamic properties of the cluster phase are constant against the density in the high-density region as $V_c/N < 30\ \sigma^3$, and the EOS would extrapolate the V_c/N in the high-density region. Possibly, in the high-density region, the density dependence that we neglected becomes remarkable; therefore the EOS would overestimate the ΔG. On the contrary, in the low-pressure/low-density region, the EOS of ΔG is consistent with that of ΔA because the extrapolation is not remarkable. Figure 17 shows the behavior of the components of the nucleation energy: $\Delta U_G(N, T, P)$, $P\Delta V_G(N, T, P)$, and $T\Delta S_G(N, T, P)$ of the ΔG, besides $\Delta U_A(N, T, V)$ and $T\Delta S_A(N, T, V)$ of the ΔA.

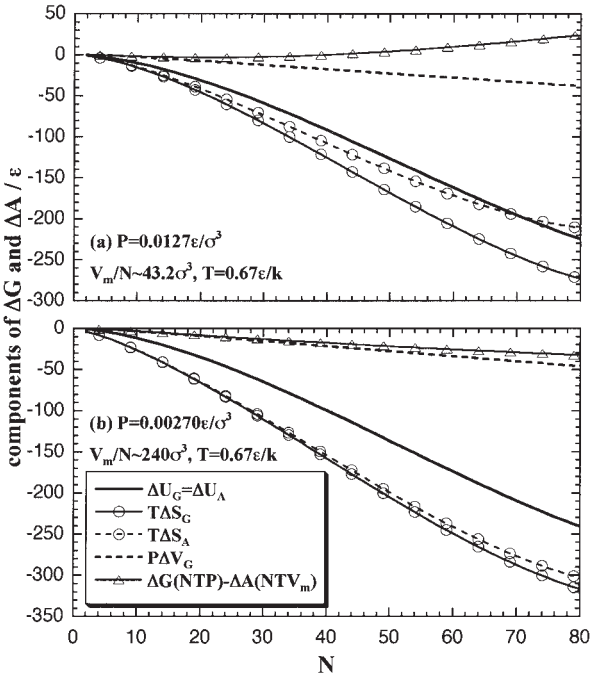

Fig. 17. Components of ΔG and ΔA. In the high-pressure system (a), the difference $T\Delta S_G - T\Delta S_A$ becomes remarkable with the increase of N, which negates the negative contribution of the $P\Delta V_G$ and raises the ΔG. On the other hand, the low-pressure (b), the difference between the entropy terms becomes smaller, therefore the difference $\Delta G - \Delta A$ is almost occupied by the $P\Delta V_G$ contribution and the ΔG becomes lower than the ΔA.

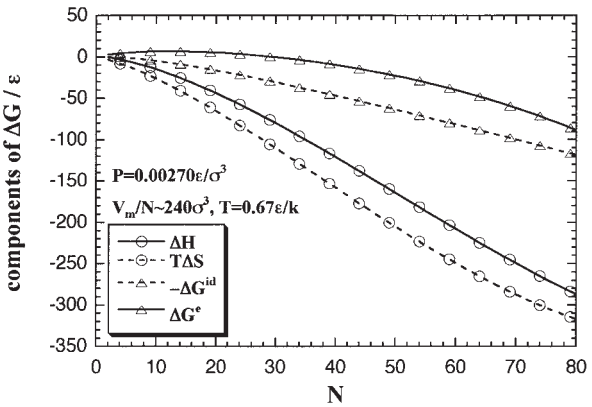

Fig. 18. Components of ΔG; ΔH and $T\Delta S$, ΔG^{id} and ΔG^{e} at $P = 0.00270\ \varepsilon/\sigma^3$, $T = 0.67\ \varepsilon/k$. The ideal gas term is plotted as $-\Delta G^{id}$.

The effect of the extrapolation in high-pressure/high-density region as in fiuure (a) is much larger than the effect in low-pressure/low-density region as in (b); the deviation of the $T\Delta S_G$ term raises the ΔG as in figure (a).

Here, we consider the reason why the ΔG curve obtains a maximum against the number of particles. The ΔG can be divided into the enthalpy term and the entropy term as in Eq. 24, and can be divided into the ideal gas term and the interaction term as $\Delta G = \Delta G^{id} + \Delta G^{e}$. The components are plotted in Fig. 18. In the small-N region, the enthalpy term or the

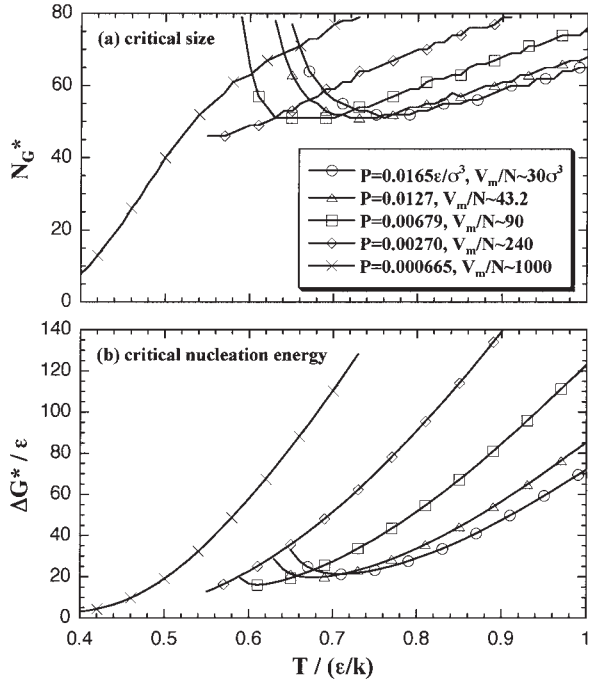

Fig. 19. The values of the critical nucleus in (N, T, P) domain: (a) the size N_G^* and (b) the Gibbs free energy ΔG^*. As we stated in the text, the both N_G^* and ΔG^* are overestimated at the high-pressure system.

interaction term (solid curves) is higher than the entropy term or the ideal gas term (dashed curves), and the slope of the former is less than that of the latter. Therefore, the ΔG has a positive value and increases against the number of particles for a while. However, after all, the enthalpy term or the interaction term overtakes the entropy term or the ideal gas term due to increase of the slope of the solid curves. Accordingly, the ΔG has a maximum as in Fig. 15. The values of the critical nucleus, the size N_G^* and the nucleation energy ΔG^*, are plotted in Fig. 19 as a function of temperature.

Comparison with Classical Theory and Other Simulations. According to the classical nucleation theory,[16] the free energy of nucleation is expressed as

$$\Delta G = \gamma A_s + \Delta g V. \tag{30}$$

Here the first term relates to surface contributions: γ is surface tension and A_s surface area of the cluster. The second term relates to bulk contributions: Δg is the free energy change per unit volume between the bulk liquid and bulk vapor phases, and V is the volume of the cluster. When the shape of cluster is spherical, A_s and V are obtained from the radius of the cluster r as $A_s = 4\pi r^2$ and $V = (4/3)\pi r^3$. The free energy change Δg is obtained as $\Delta g = -\rho_l kT \ln S$, where $S = (\rho/\rho_{sat})$ is the supersaturation ratio of the vapor phase, while ρ_l, ρ, and ρ_{sat} are the densities of the bulk liquid, the supersaturated vapor and the saturated vapor. The number of particles of the cluster is expressed as $N = \rho_l V$. Such relations allow Eq. 30 to be rearranged as a function of N, T, and S:

$$\Delta G = 4\pi\gamma\left(\frac{3N}{4\pi\rho_l}\right)^{2/3} - NkT\ln S, \tag{31}$$

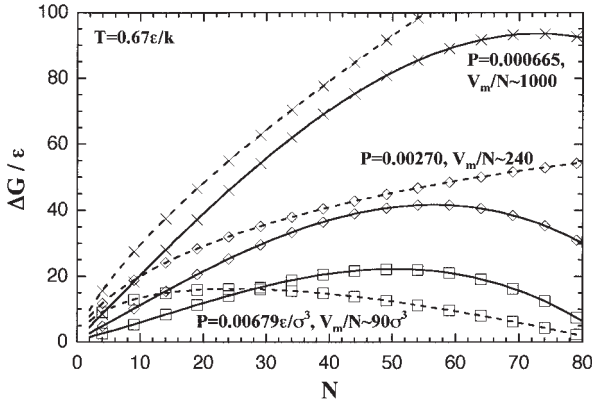

Fig. 20. Comparison between the EOS and the classical theory at $T = 0.67\ \varepsilon/k$. The former is plotted as solid curves, and the latter dashed curves.

where $\gamma = 1.03\ \varepsilon/\sigma^2$, $\rho_l = 0.82\ \sigma^{-3}$, and $\rho_{\mathrm{sat}} = 0.00161\ \sigma^{-3}$ at $T = 0.67\ \varepsilon/k$.[5] We compared the EOS and the classical theory in Fig. 20. The classical theory overestimates the free energy of the critical nucleus ΔG^*, and underestimates the size of the critical nucleus N_G^*; these have been reported as computational and experimental results.[17,18] Though the EOS also overestimates both ΔG^* and N_G^*, the values seem to be consistent with the inclination of the classical theory.

The nucleation free energy and the size of the critical nucleus are obtained from Eq. 31 as

$$\Delta G^* = \frac{16\pi\gamma^3}{3(\rho_l kT \ln S)^2}, \tag{32}$$

$$N_G^* = \frac{32\pi\gamma^3}{3\rho_l^2(kT \ln S)^3}. \tag{33}$$

Oh and Zeng estimated the N_G^* and ΔG^* of LJ system by MC simulations of the nucleation in a large system in which they set an upper limit of the size of cluster.[5] Yasuoka and Matsumoto performed molecular dynamics simulations for the nucleation of LJ system, and also obtained the N_G^* and ΔG^*.[1] Figure 21 shows the comparison between the results of the EOS and the other simulations. As we stated above, since the EOS overestimates the ΔG in the high-density region by the effect of the extrapolation of the V_c/N, the reliability of the EOS is low in the high-density region. Yet, it can be expected that the EOS will give a suitable prediction except for the region where the N^* and the ΔG^* rise against density increase, ca. $V_m/N < 60\ \sigma^3$.

In the classical theory, Eq. 30, the ΔG gives a maximum against the cluster size due to competition between the surface and the bulk contributions. The classical theory is a prediction from the macroscopic phenomenology. On the other hand, in the EOS from the microscopic MC simulations, the maximum is obtained from the competing between the enthalpy and the entropy term or the interaction and the ideal gas term, as stated above. The model proposed in this study daringly simplified the N-particle nucleation as monomer-cluster transition in an N-particle system. Still the model gave the maximum values of ΔG (and ΔA) near to the prediction of the classical theory, and was qualitatively consistent with the classical theory. The agreement suggests that, though more examinations are required, the model is available to predict the nucleation energy.

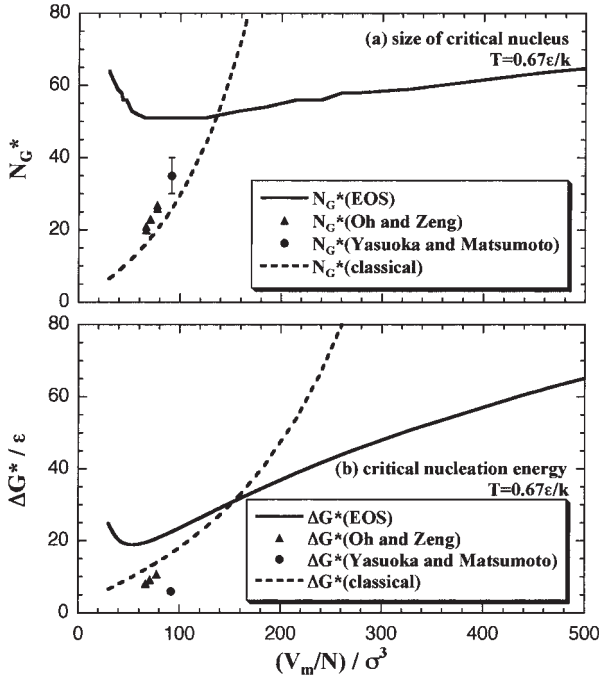

Fig. 21. Comparison with other simulations in the values of the critical nucleus at $T = 0.67\ \varepsilon/k$. The triangles and circles are the results from other simulations.[1,5] The prediction of the classical theory is also plotted.

Conclusion

We carried out Monte Carlo simulations for homogeneous nucleation in supersaturated Lennard-Jones vapor phase to estimate the free energy of the nucleation. The nucleation energy is obtained as the differences between the free energies of cluster and monomer phases. The free energies of each phase are obtained independently. During the simulation for the cluster phase, we adopted Stillinger's cluster criterion to restrict all the particles of the system as a unified cluster over the whole range of simulated temperature. On the other hand, we got the monomer phase as the decomposed cluster by heating calculation, and used the thermodynamic properties of the monomer phase at the high temperature as those for the whole range of temperature. We set the number of particles at 2–80 and the volume per particle 30–1000 σ^3; MC simulations are performed on 128 states.

The obtained MC results were arranged as an equation of state of Helmholtz free energy of the nucleation that depends on the number of particles, temperature, and volume per particle. The approximation was performed by the least-squares fitting. Moreover, we rearranged the EOS for the Gibbs free energy ΔG as a function of the number of particles, temperature, and pressure. The EOS for ΔG overestimated the nucleation energy in the fairly high-supersaturated region, yet, except for that region, the EOS predicts ΔG adequately as regards tendency.

This work is supported in part by a Grant-in Aid for Scientific Research (No. 12640504) from the Ministry of Education, Culture, Sports, Science and Technology. The authors thank

the Super Computer Center, Institute for Solid State Physics. The authors thank the Research Center for Computational Science for the use of super computer. Some computation was also done at Computational Science Research Center, Hosei University.

References

1 K. Yasuoka and M. Matsumoto, *J. Chem. Phys.*, **109**, 8451 (1998).
2 K. Yasuoka, Ph. D. Thesis, Nagoya University (1997).
3 P. R. ten Wolde and D. Frenkel, *J. Chem. Phys.*, **109**, 9901 (1998).
4 P. R. ten Wolde and D. Frenkel, *J. Chem. Phys.*, **109**, 9919 (1998).
5 K. J. Oh and X. C. Zeng, *J. Chem. Phys.*, **110**, 4471 (1999).
6 K. J. Oh and X. C. Zeng, *J. Chem. Phys.*, **112**, 294 (2000).
7 I. Kusaka and D. W. Oxtoby, *J. Chem. Phys.*, **110**, 5249 (1999).
8 Y. Kataoka and Y. Yamada, *Fluid Phase Equilib.*, **194–197C**, 207 (2002).
9 Y. Yamada and Y. Kataoka, *Bull. Chem. Soc. Jpn.*, **76**, 81 (2003).
10 J. M. Haile, "Molecular Dynamics Simulation: Elementary Methods," Wiley Interscience, New York (1992).
11 F. H. Stillinger, *J. Chem. Phys.*, **38**, 1486 (1963).
12 Y. Kataoka and M. Matsumoto, *Bull. Chem. Soc. Jpn.*, **70**, 1795 (1997).
13 F. H. Ree, *J. Chem. Phys.*, **73**, 5401 (1980).
14 F. F. Abraham and J. A. Barker, *J. Chem. Phys.*, **63**, 2266 (1975).
15 W. Miehle, O. Kandler, T. Leisner, and O. Echt, *J. Chem. Phys.*, **91**, 5940 (1990).
16 A. Laaksonen, V. Talanquer, and D. W. Oxtoby, *Annu. Rev. Phys. Chem.*, **46**, 489 (1995).
17 X. C. Zeng and D. W. Oxtoby, *J. Chem. Phys.*, **94**, 4472 (1991).
18 C. Hung, M. J. Krasnopolar, and J. L. Katz, *J. Chem. Phys.*, **90**, 1856 (1989).